Optimization of Nonreciprocal Transmission Through Dissipative Phononic Crystals With Machine Learning Techniques

DMITRII SHYMKIV[1], ARNAV MAZUMDER[1,2], JESÚS ARRIAGA[3], AND ARKADII KROKHIN[1]

[1]Department of Physics, University of North Texas, Denton, TX 76203, USA
[2]Department of Mathematics, University of Washington, Seattle, WA 98195, USA
[3]Instituto de Física, Universidad Autónoma de Puebla, Puebla 72570, Mexico
CORRESPONDING AUTHOR: A. KROKHIN (arkady@unt.edu)

ABSTRACT Transmission through a phononic crystal of metallic rods in a viscous environment is numerically calculated. The cross-section of the rods is selected to be asymmetric to provide very different transmission in opposite directions along a given crystallographic line. Difference in transmission contains the reciprocal part, caused by asymmetry of the scatterers, and the truly nonreciprocal part, related to nonequal viscous losses for sound waves propagating in opposite directions. The rectification ratio for different levels of asymmetry is evaluated and optimized over its value at a fixed frequency, with various machine learning models. The possibility of using asymmetric phononic crystals as acoustic diodes is discussed.

INDEX TERMS Nonreciprocal transmission, phononic crystal, viscous dissipation.

I. INTRODUCTION

RECIPROCITY in the propagation of a monochromatic acoustic wave through a set of solid scatterers is traditionally formulated for pressure $p_B(r_A)$ measured at a point r_A when the source of sound is at point r_B. According to the Rayleigh theorem [1], switching the positions of the emitter and receiver conserves pressure,

$$p_B(r_A) = p_A(r_B). \qquad (1)$$

Originally, the reciprocity theorem was demonstrated for an inviscid fluid, where the field of acoustic velocities is potential, $\nabla \times v_{ac} = 0$. However, it remains true even in viscous media, where velocity acquires a solenoidal part, $v = v_{ac} + v_{vor}$. The distribution of velocities $v(r)$ is a solution of the wave equation obtained from the Navier-Stokes equation where pressure is excluded using the continuity equation. The distribution of pressure is obtained from the linearized continuity equation, which yields

$$p(r) = -\frac{ic^2 \rho}{\omega} \nabla \cdot v, \qquad (2)$$

where c is the speed of sound, ρ in the fluid density, and $\omega/2\pi$ is the wave frequency. Since $\nabla \cdot v_{vor} = 0$, pressure is defined only by the potential part of velocity, and the reciprocity relation (1) is also satisfied in a viscous fluid.

Reciprocity in fluid dynamics originates from time-reversal symmetry (T symmetry) of the Euler equation. While viscous dissipation breaks T symmetry, making fluid dynamics irreversible, dissipation is not considered as a factor of nonreciprocity in modern literature [2] and [3] since relation (1) remains true. So, is there a measurable quantity which becomes nonreciprocal due to viscous losses? The answer is yes: sound intensity, $I = pv$.

In an ideal (inviscid) fluid pressure serves as potential for acoustic velocity, $v(r) \propto \nabla p(r)$. The reciprocity of pressure does not mean the same symmetry for its gradient, i.e., $v_A(r_B) \neq v_B(r_A)$, since this kind of reciprocity does not mean that pressure as a function of coordinates is either even or odd. This asymmetry of velocity is consistent with time-reversal symmetry of fluid dynamics. However, this asymmetry in a viscous fluid leads to different dissipated power upon switching positions of the emitter and receiver. The local dissipation is defined by the binary combinations of velocity gradients $(\partial v_i / \partial x_k)^2$ [4]. Asymmetry in a distribution of local velocities and their gradients leads to a difference in the total dissipated power [5], [6]. The difference in attenuation of the signal on the way from the emitter to receiver is a source of dissipation-induced nonreciprocity. Indeed, the replacement $t \rightarrow -t$ and $\eta, \xi \rightarrow -\eta, -\xi$
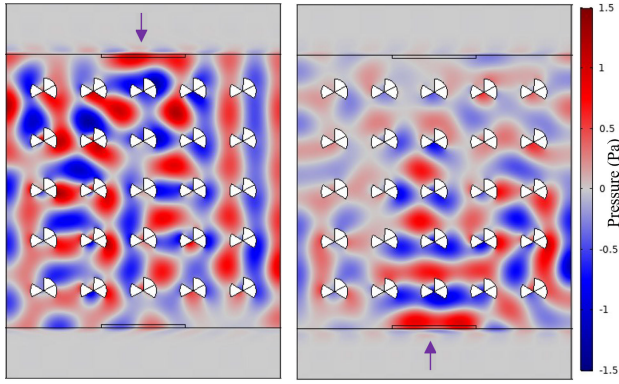
FIGURE 1. Pressure maps calculated for the crystal with asymmetrical scatterers and ideal fluid for downward (left) and upward (right) wave propagation. The difference in pressure is due only to the asymmetric transmission.

TABLE 1. Material properties of water and aluminum used in the numerical simulations.

Material	Density, kg/m³	Young's Modulus, GPa	Poisson's Ratio	η, mPa·s	ξ, mPa·s	Compressibility, 10⁻¹⁰/Pa
Water	1000	-	-	1.04	3.38	4.6
Aluminum	2700	69.14	0.33	-	-	-

does not restore the initial state of the signal, where η and ξ are the viscosity coefficients. Of course, a case of mirror symmetry in a distribution of scatterers can be excluded. In this special case, the transmission is irreversible and reciprocal. In what follows, we consider scatterers without mirror symmetry, when the P symmetry (parity symmetry) of the system is broken. The difference in sound intensities, $I_{AB} = I_A(r_B) - I_B(r_A) = \Delta I_{AB}^{ac} + \Delta I_{AB}^{nr}$ has two different contributions. The asymmetric part, ΔI_{AB}^{ac}, exists even in an inviscid fluid if P symmetry is broken. For the reference, Figure 1 shows asymmetrical pressure distributions for the forward and backward wave propagation in the case of inviscid fluid. The truly nonreciprocal part, ΔI_{AB}^{nr}, is due to broken PT symmetry. The relation between these contributions depends on viscosity, which is a measure of the violation of T symmetry.

Difference between forwards and backwards transmission may be explored for the rectification of acoustic signals and noise control [9], [10], [11]. While in a linear system the asymmetry may be a useful property that allows for the aforementioned applications. The presence of unbroken T symmetry and reciprocal transmission means that they are not true acoustic diodes [12]. Here, we propose a phononic crystal with highly asymmetric aluminum rods in viscous water, which serves as a passive acoustic diode. The design of the phononic crystal was optimized using machine learning methods to reach the best performance. In order to perform optimization, Deep Learning, a class of machine learning models, is used due to its unparalleled efficiency in modelling highly nonlinear data. Although these models primarily focus on generating accurate predictions from data, they can also be used to obtain extreme or optimal values that are not present in the original dataset. Other popular methods of optimization involve genetic or evolutionary algorithms. However, these methods require a large number of time-consuming numerical calculations at each generational step. On the other hand, in the Deep Learning approach, once a dataset

is calculated, a model can be trained and optimized to find the best parameters, which potentially reduces computational time. Deep Learning is widely used in similar problems in optimization of the properties of metasurfaces [7] and nanostructures [8].

Since the rectification ability of an acoustic diode with respect to intensity is partially due to asymmetry and partially to dissipation-induced nonreciprocity, it belongs neither to the class of reciprocal sound rectification devices [9], [10], [11], nor to completely nonreciprocal acoustic diodes [13], [14], [15], [16]. Note that the dissipation-induced mechanism of nonreciprocity was already explored in the rectification of elastic waves [17].

II. THE PHONONIC CRYSTAL AND DATA COLLECTION
We calculate the transmission spectra of a phononic crystal of aluminum rods with an asymmetric cross-section submerged in water. A typical 5×5 sample of a phononic crystal is shown in Fig. 2. All the relevant material parameters are provided in Table 1. We quantify acoustical nonreciprocity in a phononic crystal using the forwards T_F and backwards T_B sound transmission through the crystal. The following physical quantities: nonreciprocity NR

$$NR = (T_F - T_B)_{vis} - (T_F - T_B)_{id} \quad (3)$$

normalized nonreciprocity (NNR)

$$NNR = \left(\frac{T_F - T_B}{max(T_F, T_B)}\right)_{vis} - \left(\frac{T_F - T_B}{max(T_F, T_B)}\right)_{id} \quad (4)$$

and diode efficiency

$$F = \left(\frac{min(T_F, T_B)}{max((T_F, T_B)}\right)_{vis} \quad (5)$$

have been optimized. Here subscript *vis* refers to the transmission calculated for the viscous water, while *id* transmissions is calculated for the inviscid water, where $\xi = \eta = 0$. In Eq.(3), $(T_F - T_B)_{vis}$ is the total difference in the transmission, which includes asymmetric and nonreciprocal parts, while $(T_F - T_B)_{id}$ is the reciprocal part caused only by asymmetry. We would like to maximize the magnitude of both NR and NNR. In Eq.(5), F is in the range between 0 and 1. In an ideal acoustic diode, $F = 0$, which means that it allows for the propagation of sound only in one direction. Therefore, the closer F is to 0 the better the corresponding crystal performs as a diode.

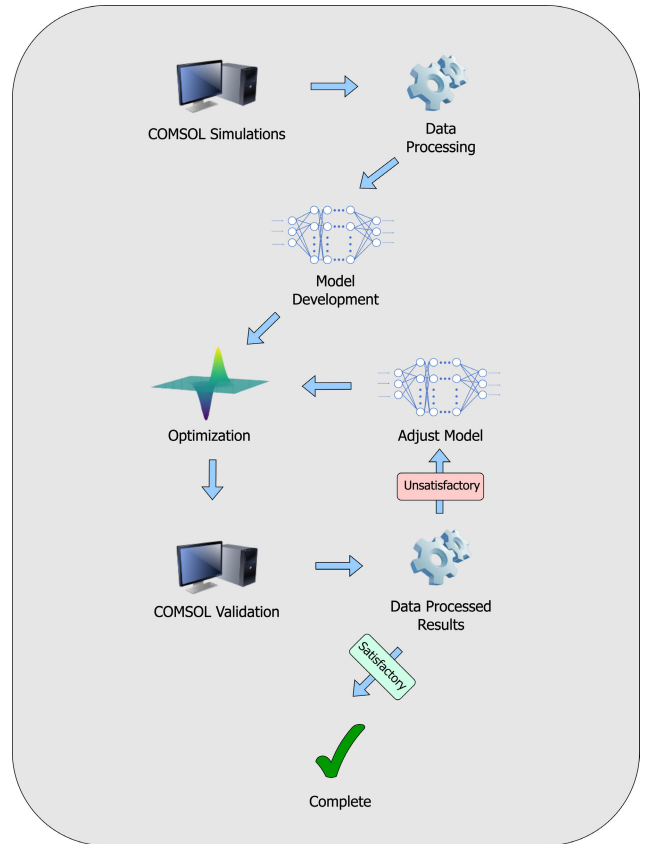Any machine learning model requires some set of data to train on and then evaluate its performance with. For these
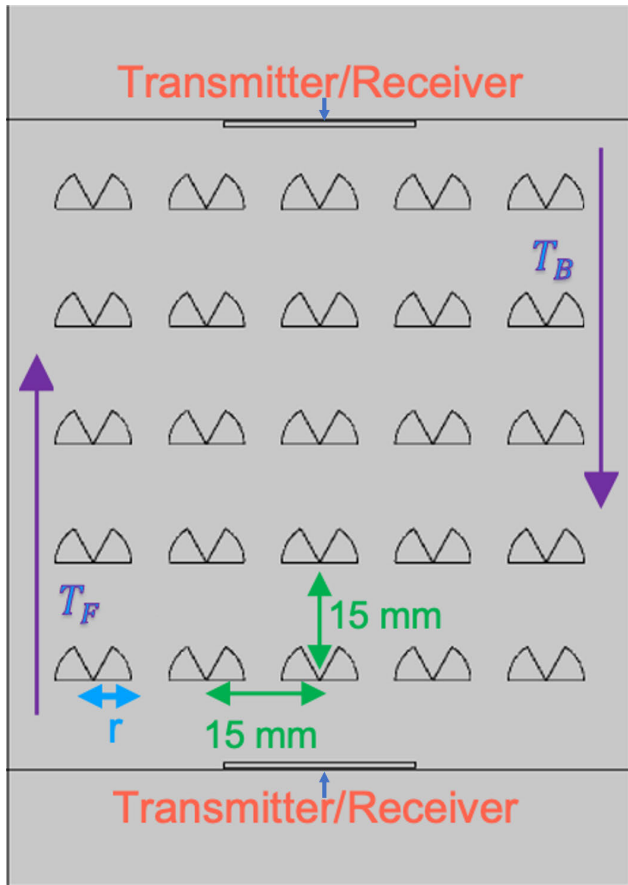
FIGURE 2. A model of the 5 x 5 2D phononic crystal used in the COMSOL calculations of the transmission spectra. The crystal consists of aluminum scatterers in a water background. Solid Mechanics and Linearized Navier-Stokes moduli were used for calculations of elastic and acoustic fields in the sample. The transmitter and receiver are placed either above or below the structure. The period of the crystal is $a = 15mm$. The sound hard boundary condition is imposed for the left and right boundaries. All external domains are perfectly matched layers (PML). Sound transmission in the forwards (T_F) and backwards (T_B) directions are numerically calculated for viscous and inviscid water.

FIGURE 3. Optimization pipeline.

FIGURE 4. Unit cells of the phononic crystal with varying scatterer sector angle. Period is 15 mm; sector radius is 6 mm; sector angle is 10°(left), 120°(middle), 300°(right).
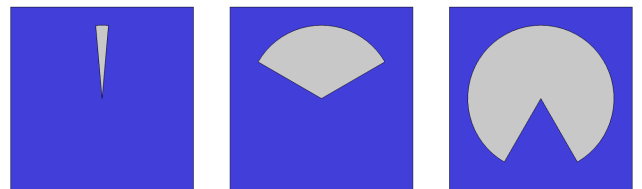
purposes, the transmission values at frequency 100 kHz are calculated for a number of phononic crystals with different cross-sections of the scatterers using COMSOL Muliphysics. Various geometrical parameters of the scatterers of the crystal are parametrically swept in COMSOL, and the corresponding sound transmission values, in the forwards and backwards directions, are recorded. These simulations are run both with the phononic crystal submerged in viscous and inviscid water. Once all desired transmission spectra are calculated, a standard optimization pipeline (see Fig. 3) is applied.

III. SINGLE PARAMETER OPTIMIZATION
As a prototype for a scatterer geometry, a rod with a sector angle of 120° [5] was chosen. A reasonable generalization valid for optimization is a sector with variable angle. As the

first step of optimization the transmissions are calculated for 171 different sector angles in the range between 5° and 345° with a step of 2°(Fig. 4). Angles less than 5° and exceeding 345° are not considered since they are near-symmetrical in shape and because of high resolution requirements in mesh creation in COMSOL.
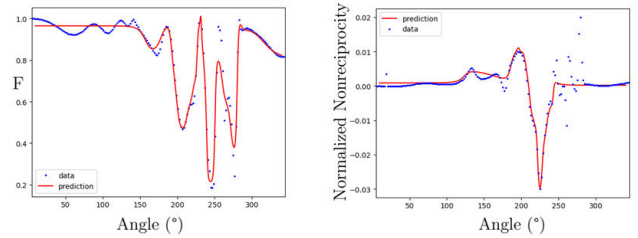
From the dataset, it was found that the configuration with the highest nonreciprocity value, *NR*, corresponds to an angle of 243°. However, a Deep Neural Network (DNN) model is believed to provide an angle with a higher nonreciprocity value. Firstly, normalization and division of the initial dataset into training (60%), testing (20%), and validation (20%) sets was performed. Then a simple neural network with 2 hidden layers and 35 nodes each was trained with features as angles and labels as nonreciprocity values. Training and validation losses as functions of the number of epochs (learning curves)
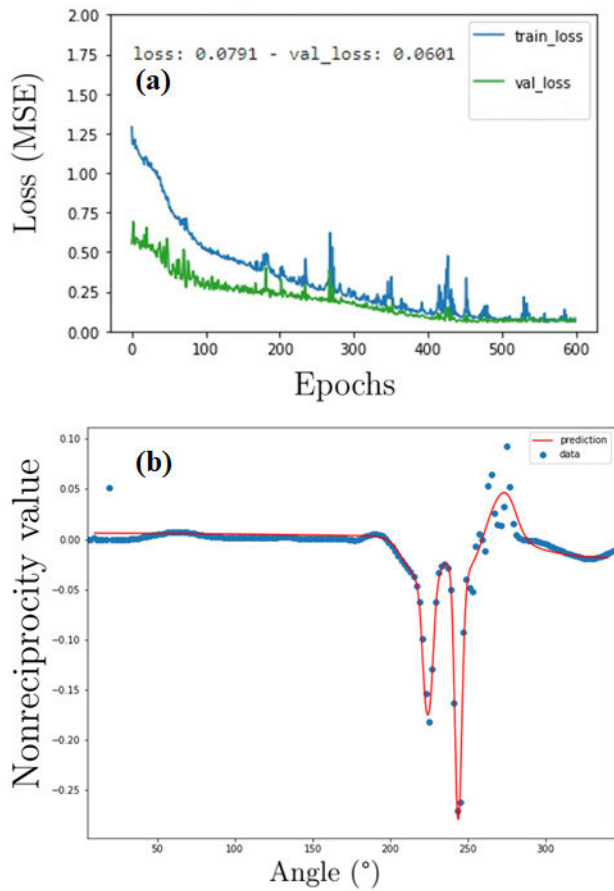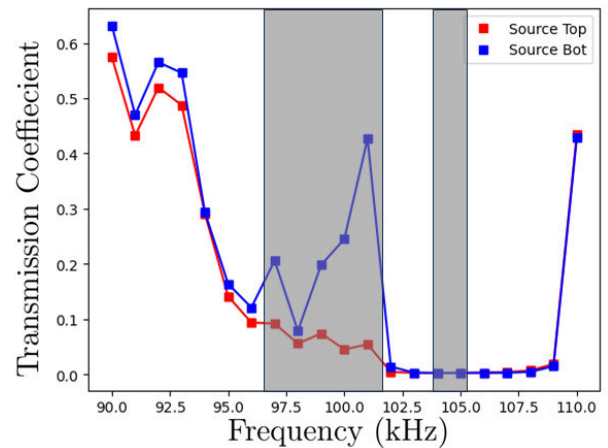
FIGURE 5. (a) Loss (mean squared error) as a function of the number of epochs for the *NR* optimization model. (b) Original data points and predictions made with a DNN model for the optimization of *NR*.

FIGURE 6. Original data points and predictions made with a DNN model. Left pannel: Optimization for *F*. Right pannel: Optimization for *NNR*.

FIGURE 7. Transmission spectra for the 5 x 5 phononic crystal sample in viscous water with the parameters corresponding to the best *F*- value. Downward propagation ("Source Top") is shown with red color, while upward propagation ("Source Bot") is depicted with blue color. The top/bottom positions of the source are indicated in Fig. 2. The shaded areas are the regions of the band gaps in the infinite phononic crystal with inviscid water. Note that the narrow transmission region between the gaps is not resolved for the finite-size sample.

FIGURE 8. Ten different asymmetric cross-sections of scatterers.

show no overfitting. The sector angle with the highest non-reciprocity from model predictions is 243.7165°, which is a 3.4% (0.279 a.u.) increase in nonreciprocity compared to the highest value from the original dataset (Fig. 5). Direct transmission calculations with this sector angle using COMSOL confirm that nonreciprocity is higher (0.382 a.u.) than that obtained in the original dataset. Although the calculated non-reciprocity is not identical to the predicted one, the predicted sector angle provides a higher nonreciprocity value. Finally, using this optimization method, we obtained a nonreciprocity value that is more than 40% higher than the highest value from the initial dataset.
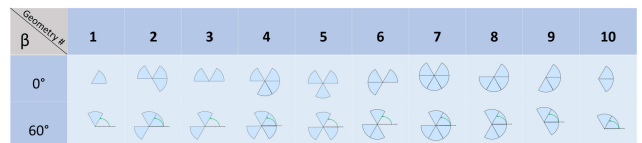
Similarly, by adjusting the model parameters to reach a lower loss (mean squared error) and avoid overfitting, the optimized sector angles are found for normalized nonre-ciprocity and diode efficiency. Predictions in Figs. 5 and 6 do not have a one-to-one correspondence with points from the datasets, especially when fluctuations are small and rapid. For the values of *NNR* and *F*, optimal predictions from the model may not be better than the best values obtained from the original dataset. However, the angles at which these

models predict to have optimal values do indeed exhibit better values than those from the original dataset, and COMSOL calculations validate the correctness of these models, see Table 2.

To analyze the effectiveness of the acoustic diode repre-sented by a 5 × 5 sample with the parameters corresponding to the best *F*-value, the transmission spectra in viscous water as well as the band structure for the corresponding infi-nite crystal with inviscid water are calculated. The results for the region of frequencies near 100 kHz are represented by Fig. 7.
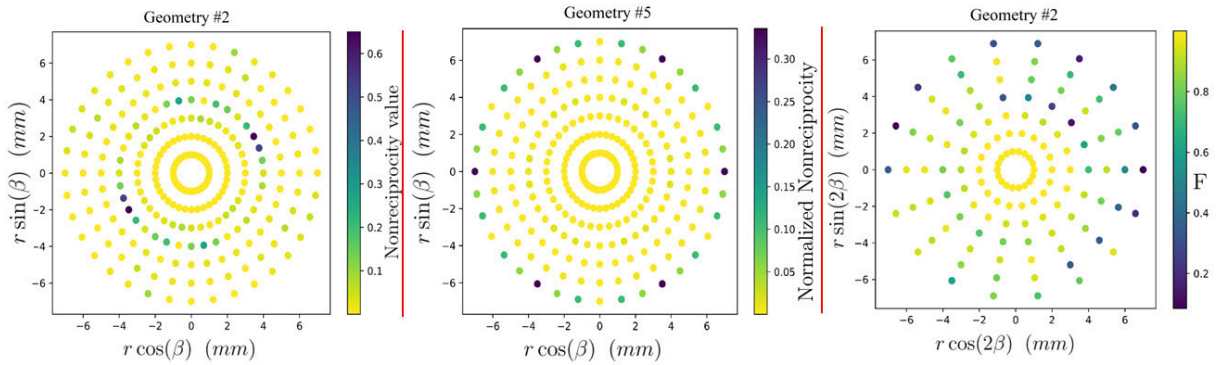
FIGURE 9. Original data for the geometry types with the highest *NR* (left), *NNR* (center) and the lowest *F* (right).

TABLE 2. The best nonreciprocity *NR* (maximizing), normalized nonreciprocity *NNR* (maximimzing), and diode efficiency *F* (minimizing) from the dataset with model predictions and COMSOL validated values for the optimized parameters.

Method	NR (a.u.)	Angle (deg)	NNR (%)	Angle (deg)	F (%)	Angle (deg)
Dataset	0.27	243	2.99	225	18.5	247
Prediction	0.279	243.7165	2.97	225.1017	21.2	245.5978
COMSOL Validation	0.382	243.7165	3.01	225.1017	18.4	245.5978

TABLE 3. The highest (lowest for *F*) nonreciprocity, normalized nonreciprocity and diode efficiency from the dataset.

	NR (a.u)	NNR (%)	F (%)	F (%) Extended
Dataset	0.65	33.5	8.48	5.52
β (°)	30	0	0	180
r (mm)	4	7	7	7.2
Geometry Type				

Since the 100 kHz frequency lies within the band gap, the transmission in the infinite crystal is zero in both directions. Moreover, it was shown in Ref. [6] that the dispersion relation, being a complex function in a viscous environment, remains an even function $\omega(k) = \omega(-k)$, i.e., the dissipation-induced nonreciprocity is a finite-size effect which gradually disappears with sample length. Due to the finite size of the crystal, viscosity of water, and sound hard boundaries on the left and right boundaries of the finite crystal, the asymmetry in the transmission is clearly manifested. For one direction (downward, when source is above the crystal) of the wave propagation, the transmission coefficient is high enough to detect it. For the other direction (upward, when source is below the crystal), there is a good suppression of the sound intensity, which indicates blocking a signal. Moreover, an even better value for *F* can be achieved at 101 kHz where $F = 12.7\%$ and the transmission coefficient of the acoustic diode in the forward direction exceeds 40%.

IV. MULTIPLE PARAMETERS OPTIMIZATION

The next step in the generalization of a prototype is to consider asymmetric scatterers composed of several sectors of 60° each with variable radius *r* and variable orientation of the sector characterized by angle *β*. Ten different geometries shown in Fig. 8 were analyzed. The angle *β* characterizes orientation of the scatterer as a whole. In Fig. 8 the rotation by angle *β* is shown for the cross-sections (1) and (10). All other scatterers are displaced for $\beta = 0$.

The original dataset is created calculating transmissions for each type of geometry with a radius in the range of 1 mm and

7 mm with a step of 1 mm and with a rotational angle in the range of 0° and 180° with a step of 10°. The limitation for the radius is due to the size of the unit cell ($a = 15 mm$). The geometries with angles $180° < \beta < 360°$ do not provide any new information about the transmission coefficient and are, therefore, not numerically calculated in COMSOL. More than 5000 transmission values are calculated including those for viscous and inviscid water in the upward and downward directions. For visualization and predictions, a polar representation is chosen which accounts for the periodic behavior of the data (Fig. 9). In this approach, $\cos\beta$ and $\sin\beta$ are considered as features along with the radius *r* for *NR* and *NNR* models. Since the *F*-value function has a period of π (Eq. 5), double angled trigonometric functions are used.

Examining Fig. 9 (right), it is evident that we might expect even lower *F*-values for higher radii of the scatter. Additional data was calculated for $r = 7.2$ mm and $r = 7.4$ mm using COMSOL and included in the extended dataset (Table (3)).

Using a similar approach as in Section III, the values for *NR*, *NNR*, and *F* are predicted for all possible *r* and *β* values in the range between 1 mm and 7 mm (7.4 mm for *F*) for the radius and 0° and 180° for the angle (Fig. 10). DNN models for *NNR* were either underfitted (provide poor predictions with training data) or overfitted (cannot be used for new predictions). In other words, because the highest *NNR* value (33.5%) is much greater than the remaining data, all tested machine learning models either considered it an outlier

TABLE 4. The highest (lowest for F) nonreciprocity, normalized nonreciprocity and diode efficiency from the dataset and predictions as well as 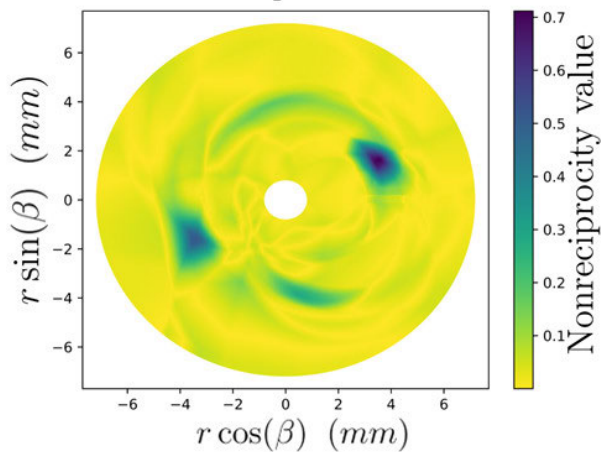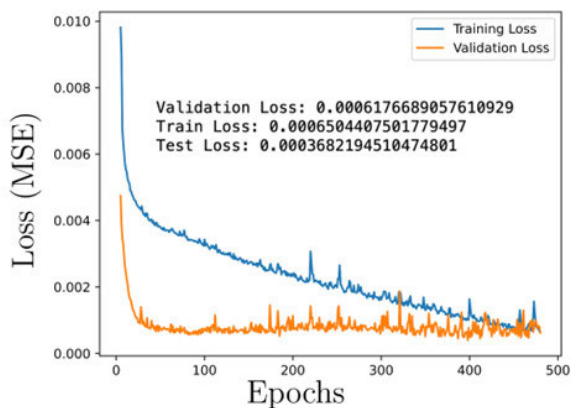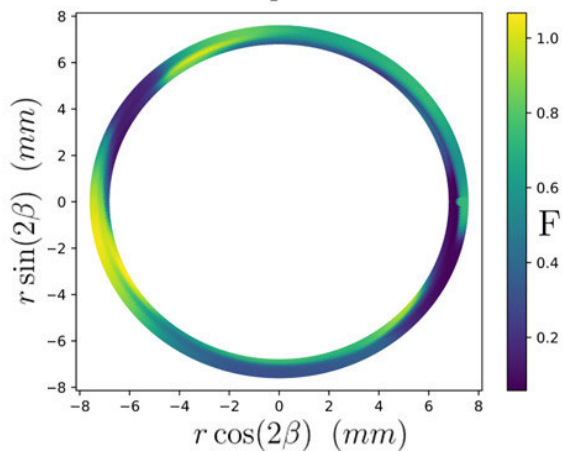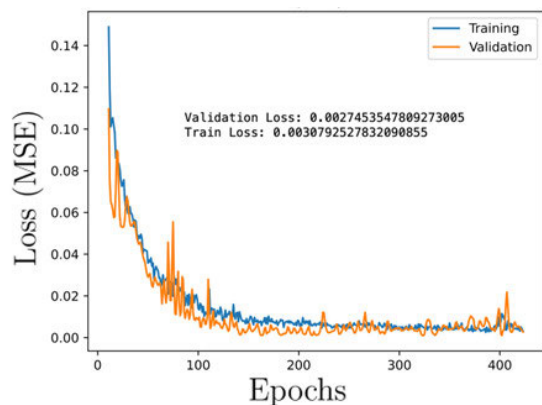COMSOL validated values for the optimized parameters. The best values are highlighted and the corresponding radius and rotation angle are provided.

	NR (a.u)	NNR (%)	F (%)	F (%) Extended
Dataset	0.65	**33.5**	**8.48**	5.52
Prediction	0.71	8.91	-	5.88
COMSOL Validation	**0.70**	13.3	-	**5.30**
β (°)	27.7444	0	0	0
r (mm)	3.9657	7	7	7.1966
Geometry Type				

FIGURE 11. Diode efficiency optimization. Loss (mean squared error) as a function of a number of epoch (top) and predictions of the DNN models of F (bottom). The model consists of 5 hidden layers with 1000 nodes and a 15% dropout rate in each layer.

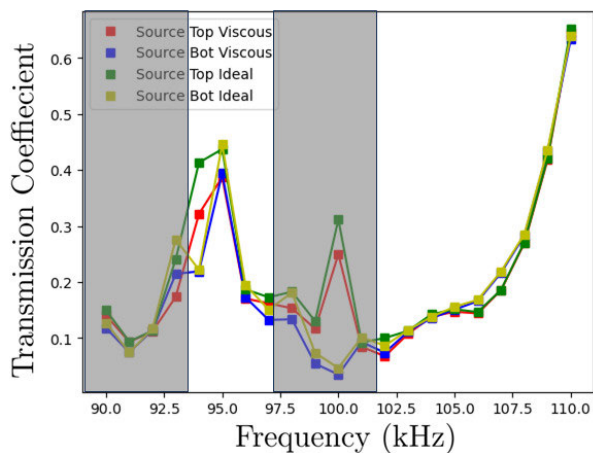
FIGURE 10. Nonreciprocity optimization. Loss (mean squared error) as a function of a number of epoch (top) and predictions of the DNN models of NR (bottom). The model consists of 4 hidden layers with 17 nodes each.

FIGURE 12. Transmission spectra through the 5 x 5 sample with the parameters providing the highest value of nonreciprocity NR. The parameters of the scatterer are given in Table 4. Note that the narrow transmission band lying between two bandgaps (marked as shaded areas) is well-resolved, unlike similar transmission band in Fig. 8.

or fitted too closely to it to the point at which the model perfomed poorly on validation and testing data (unseen by the model). The 3-fold rotational symmetry in Fig. 9 (center) is due to the corresponding symmetry of the scatterer, where all maxima correspond to technically the same geometry. The model for nonreciprocity has relatively small final loss and is not overfitted. Predictions have two regions with high values that are located around 4 mm and 30 (210) degrees, which

correlates to the original data. The highest nonreciprocity prediction, which is 9% higher than the one from the dataset,

is validated with COMSOL. Direct calculations prove the correctness of the model (Table 4).

After optimization of the diode (Fig. 11), it is found that the lowest F-value is 5.3%, which means that the ratio of the transmissions in the forward and reverse direction is almost 20. The calculated transmission spectra for the optimized 5×5 sample are shown in Fig. 12. Just like the spectra in Fig. 7, the best contrast between the forward and reverse transmission lies within the bandgap calculated for the corresponding infinite crystal. This is one more manifestation of asymmetry, which means that the destructive interference leading to the formation of a bandgap in an infinite crystal is sensitive to the direction of wave propagation (forward or reverse). Of course, the asymmetry vanishes with the size of the sample, but for the finite-length samples it may be explored for the rectification of acoustic signals. In particular, the phononic crystal with the parameters given in the last column of Table 4 can be used as an acoustic diode at 100 kHz.

V. CONCLUSION

In conclusion, we calculated the transmission for a 5×5 phononic crystal with different shapes of scatterers placed in a waveguide and optimized the scatter geometry to achieve the highest nonreciprocity, normalized nonreciprocity and diode efficiency. It is shown that viscosity-induced nonreciprocity strongly depends on the shape of scatterers. Its contribution to the transmission difference between the forward and backward wave propagation is comparable to the reciprocal contribution due to asymmetry, which exists in an ideal fluid background. The asymmetric and nonreciprocal contributions to the transmission may mutually enhance or weaken each other. The geometry of the scatterers when these contributions enhance each other along one direction and weaken along the opposite direction is obtained at a given frequency of 100 kHz and validated with COMSOL software. This geometry is optimal for the sample to serve as a linear non-resonant passive acoustic diode. Although the highest transmission coefficient is essentially lower than 1, it is sufficient for secure signal transmission in the forward direction and strongly suppressed signal transmission in the reverse direction. A passive acoustic diode with higher transmission in the forward direction at a resonant frequency was proposed in Ref. [11]. The high asymmetry in transmission is achieved due to different symmetry (even/odd) of the eigenmodes propagating on the left and right wings of the proposed elastic waveguide. For active acoustic diode the transmission in the forward direction may be close to 1 due to the presence of external sources of energy [13]. In a passive nonlinear acoustic diode, the transmission may be close to one since the samples are relatively short and the rectification is due to the nonlinearity of the material [18]. With a machine learning approach of optimization we were able to slightly adjust scatterer's geometry to predict and achieve parameters for better values of NR, NNR, and F. When the best values from

the original dataset are outliers (a big difference between its closest neighbors), models exhibit underfitting or overfitting. However, if the data distribution is relatively even, we get an improvement in the corresponding quantities. Our final data shows that the best values of NR, NNR and F are achieved, when the corresponding frequency is close to the edge of the band gap calculated for the corresponding infinite crystal and inviscid environment. The proposed structure may be used as a passive acoustic diode, serving without an external source of energy.

REFERENCES

[1] J. W. Strutt, "On the application of the principle of reciprocity to acoustics," *Proc. Roy. Soc. London*, vol. 25, p. 118, Jan. 1876, doi: 10.1098/rspl.1876.0025.

[2] R. Fleury, D. L. Sounas, M. R. Haberman, and A. Alù, "Nonreciprocal acoustics," *Acoust. Today*, vol. 11, p. 14, Mar. 2015.

[3] H. Nassar et al., "Nonreciprocity in acoustic and elastic materials," *Nature Rev. Mater.*, vol. 5, no. 9, pp. 667–685, Jul. 2020, doi: 10.1038/s41578-020-0206-0.

[4] L. D. Landau and E. M. Lifshitz, *Fluid Mechanics*, 2nd ed. Oxford, U.K.: Elsevier, 1984.

[5] E. Walker et al., "Nonreciprocal linear transmission of sound in a viscous environment with broken P symmetry," *Phys. Rev. Lett.*, vol. 120, no. 20, May 2018, Art. no. 204501, doi: 10.1103/PhysRevLett.120.204501.

[6] H. Heo et al., "Non-reciprocal acoustics in a viscous environment," *Proc. Roy. Soc. A, Math., Phys. Eng. Sci.*, vol. 476, no. 2244, p. 657, Dec. 2020, doi: 10.1098/rspa.2020.0657.

[7] Z. A. Kudyshev, A. V. Kildishev, V. M. Shalaev, and A. Boltasseva, "Machine-learning-assisted metasurface design for high-efficiency thermal emitter optimization," *Appl. Phys. Rev.*, vol. 7, no. 2, Jun. 2020, Art. no. 021407, doi: 10.1063/1.5134792.

[8] I. Malkiel, M. Mrejen, A. Nagler, U. Arieli, L. Wolf, and H. Suchowski, "Plasmonic nanostructure design and characterization via deep learning," *Light, Sci. Appl.*, vol. 7, no. 1, p. 60, Sep. 2018, doi: 10.1038/s41377-018-0060-7.

[9] X. Zhu, X. Zou, B. Liang, and J. Cheng, "One-way mode transmission in one-dimensional phononic crystal plates," *J. Appl. Phys.*, vol. 108, no. 12, Dec. 2010, Art. no. 124909.

[10] Y.-F. Zhu, X.-Y. Zou, B. Liang, and J.-C. Cheng, "Acoustic one-way open tunnel by using metasurface," *Appl. Phys. Lett.*, vol. 107, no. 11, Sep. 2015, Art. no. 113501.

[11] J. Zhu, X. Zhu, X. Yin, Y. Wang, and X. Zhang, "Unidirectional extraordinary sound transmission with mode-selective resonant materials," *Phys. Rev. Appl.*, vol. 13, no. 4, Apr. 2020, Art. no. 041001, doi: 10.1103/physrevapplied.13.041001.

[12] A. Maznev, A. Every, and O. Wright, "Reciprocity in reflection and transmission: What is a phonon diode," *Wave Motion*, vol. 50, Jan. 2013, Art. no. 776784.

[13] B.-I. Popa and S. A. Cummer, "Non-reciprocal and highly nonlinear active acoustic metamaterials," *Nature Commun.*, vol. 5, no. 1, p. 3398, Feb. 2014, doi: 10.1038/ncomms4398.

[14] R. Fleury, D. L. Sounas, C. F. Sieck, M. R. Haberman, and A. Alù, "Sound isolation and giant linear nonreciprocity in a compact acoustic circulator," *Science*, vol. 343, p. 516, Oct. 2014, doi: 10.1126/science.1246957.

[15] C. He et al., "Acoustic topological insulator and robust one-way sound transport," *Nature Phys.*, vol. 12, no. 12, pp. 1124–1129, Dec. 2016, doi: 10.1038/nphys3867.

[16] Y. Ding et al., "Experimental demonstration of acoustic Chern insulators," *Phys. Rev. Lett.*, vol. 122, no. 1, Jan. 2019, Art. no. 014302, doi: 10.1103/physrevlett.122.014302.

[17] Y. Tanaka, Y. Shimomura, and N. Nishiguchi, "Acoustic wave rectification in viscoelastic materials," *Jpn. J. Appl. Phys.*, vol. 57, no. 3, Mar. 2018, Art. no. 034101, doi: 10.7567/jjap.57.034101.

[18] A. Darabi, L. Fang, A. Mojahed, M. D. Fronk, A. F. Vakakis, and M. J. Leamy, "Broadband passive nonlinear acoustic diode," *Phys. Rev. B, Condens. Matter*, vol. 99, no. 21, Jun. 2019, Art. no. 214305, doi: 10.1103/physrevb.99.214305.

DMITRII SHYMKIV received the B.S. degree in physics from V. N. Karazin Kharkiv National University, Kharkiv, Ukraine, in 2018. He is currently pursuing the Ph.D. degree in physics with the University of North Texas, Denton, TX, USA. His current research interests include physical acoustics, phononic crystals, and acoustic metamaterials.

ARNAV MAZUMDER received the Texas Academy of Mathematics and Science Diploma degree in computer science from the University of North Texas, Denton, TX, USA, in 2023. He is currently pursuing the B.S. degree in the applied and computational mathematical sciences with the University of Washington, Seattle, WA, USA, with a focus on data science and statistics. His current research interests include the statistical modeling of complex numerical systems, machine learning, and physics.

JESÚS ARRIAGA received the B.S. degree in physics from Universidad Michoacana, Mexico, in 1986, and the Ph.D. degree from the Universidad Complutense de Madrid, Spain, in 1992. He has been a permanent Professor at the Universidad Autónoma de Puebla, Mexico, since 1993. His research interests are the condensed matter physics, photonic and phononic crystals. He is a member of the Academia Mexicana de Ciencias.

ARKADII KROKHIN received the M.S. degree in physics from Kharkiv State University, Kharkiv, Ukraine, in 1978, and the Ph.D. degree in physics from Kiev State University, Kyiv, Ukraine, in 1983. He was a Professor of physics with Universidad Autnoma de Puebla, Puebla, Mexico, from 1992 to 2003. He has been a Professor of physics with the University of North Texas, Denton, TX, USA, since 2003, where he is currently leading the theoretical efforts as a PI of the NSF Emerging Frontier Research Initiative. His current research interests include acoustics, condensed matter physics, and complexities. He is a member of the American Physical Society.